A generalized approach to characterize optical properties of natural objects

LAURA OSPINA-ROZO[1,*,•], ANN ROBERTS[2,•] and DEVI STUART-FOX[1,•]

[1]*School of Biosciences, University of Melbourne, VIC 3010, Australia*
[2]*ARC Centre of Excellence for Transformative Meta-Optical Systems, School of Physics, University of Melbourne, VIC 3010, Australia*

To understand the diversity of ways in which natural materials interact with light, it is important to consider how their reflectance changes with the angle of illumination or viewing and to consider wavelengths beyond the visible. Efforts to characterize these optical properties, however, have been hampered by heterogeneity in measurement techniques, parameters and terminology. Here, we propose a standardized set of measurements, parameters and terminology to describe the optical properties of natural objects based on spectrometry, including angle-dependent effects, such as iridescence and specularity. We select a set of existing measurements and parameters that are generalizable to any wavelength range and spectral shape, and we highlight which subsets of measures are relevant to different biological questions. As a case study, we have applied these measures to 30 species of Christmas beetles, in which we observed previously unrealized diversity in visible and near-infrared reflectance. As expected, reflection of short wavelengths was associated with high spectral purity and angle dependence. In contrast to simple, artificial structures, iridescence and specularity were not strongly correlated, highlighting the complexity and modularity of natural materials. Species did not cluster according to spectral parameters or genus, suggesting high lability of optical properties. The proposed standardization of measures and parameters will improve our understanding of biological adaptations for manipulating light by facilitating the systematic comparison of complex optical properties, such as glossy or metallic appearances and visible or near-infrared iridescence.

ADDITIONAL KEYWORDS: beetles – iridescence – near infrared – spectrometry – specularity – structural colour.

INTRODUCTION

The way in which living organisms interact with light is fundamental to survival. This interaction gives rise to a wide range of optical effects (a term derived from the field of optics and unrelated to visual perception), such as iridescence and gloss (Shawkey & D'Alba, 2017). Optical properties are often evolutionarily labile and can be influenced simultaneously by different receivers (e.g. conspecifics, predators, prey), context and selection for different biological functions (Endler, 1990; Stuart-Fox & Moussalli, 2009; Kemp *et al.*, 2015; Cuthill *et al.*, 2017). Thus, it is useful to describe the diversity of optical properties independent of specific receivers, because animals differ greatly in their visual sensitivity (Osorio & Vorobyev, 2008; Kemp *et al.*, 2015). In addition, optical properties include wavelengths spanning the spectral range of sunlight [~280–2600 nm; not only in the 300–700 nm ultraviolet (UV)–visible (VIS) region], reflecting light at specific angles or in various regions of the spectrum at the same time (multipeaked or sigmoidal spectra), and these complex traits do not necessarily have a visual function. Being able to describe the variability in optical properties without prior knowledge of the underlying mechanism is important for exploring both their visual and non-visual functions and to understand the evolution of these traits.

Any attempt to characterize optical properties entails simplification, which depends on the measurement approach, the nature of the material and the biological

*Corresponding author. E-mail lospinarozo@student.unimelb.edu.au

question. For example, many techniques available to characterize light reflection of natural objects, such as scatterometry and microspectrophotometry (reviewed by Vukusic & Stavenga, 2009), are designed to characterize optical properties of a small region of the surface (< 1 mm) and are used in studies describing the underlying mechanism (e.g. the extensive biophotonics literature; Kinoshita *et al.*, 2002; Wilts *et al.*, 2009; Stavenga *et al.*, 2011; Vignolini *et al.*, 2013; Fu *et al.*, 2017). In contrast, studies focusing on function and evolution most commonly use spatially unresolved spectrometry to characterize macroscopic optical properties (Johnsen, 2016). This technique involves illuminating and collecting the reflected light at specific combinations of angles (Gruson *et al.*, 2019a). However, most studies measure reflection at only one geometry (e.g. both light source and collection optical fibres within a single probe are oriented at 45° relative to the sample surface), which makes it impossible to distinguish between diffuse and specular reflection (see glossary in Table 1). Diffuse reflection is produced when a surface scatters the incoming light in a similar manner across a wide range of angles, whereas specular reflection is produced when the surface reflects most of the light only at the specular or mirror angle (equal but opposite angle of illumination and reflection; Table 1). Measurement at one angle implicitly assumes that the sample is mainly diffuse (i.e. that reflectance is not angle dependent); however, biological surfaces vary continuously in the relative contribution of diffuse and specular reflection. For example, surfaces with a glossy or metallic appearance have a high proportion of specularly reflected light compared with matte or diffuse surfaces (Franklin & Ospina-Rozo, 2021; Stuart-Fox *et al.*, 2021) (Table 1). Many structural colours are also iridescent, changing hue with the viewing or illumination angle (Meadows *et al.*, 2009; Seago *et al.*, 2009; Shawkey *et al.*, 2009; Stuart-Fox *et al.*, 2021). Angle-dependent effects, such as gloss (Table 1) and iridescence, can be characterized only with angle-resolved spectral measurements (Cuthill *et al.*, 1999; Osorio & Ham, 2002; Meadows *et al.*, 2011). Currently, however, most studies that measure reflection at more than one angle use angles that are not comparable or do not attempt to quantify angle dependence (Gruson *et al.*, 2019a).

Gruson *et al.* (2019a) proposed an effective and straightforward method to characterize the angle-dependent effects of structural colours using spectrometry with an optimized set of geometries and five parameters: hue, angle dependence of hue, maximum brightness, tilting and angle dependence of brightness. Their method was derived from the optical theory of multilayers and was used to quantify diversity in iridescent hummingbird feathers and butterfly wings (Gruson *et al.*, 2019a). Gruson *et al.* (2019a)

suggested that their parameters could be generalizable to characterize angle dependence produced by other mechanisms. However, the spectral profiles produced by ideal or almost ideal (in birds and butterflies) multilayers are characterized by isolated distinct peaks. Some modifications or additions to the parameters are needed, therefore, in order to describe angle dependence in natural materials that produce other spectral shapes, including sigmoidal shapes without peaks, broadband spectra and spectra with multiple peaks.

A variety of parameters exist to describe the shape of reflectance spectra. These have been described in various important sources (Montgomerie, 2006; Kemp *et al.*, 2015; Gruson *et al.*, 2019a) and can be implemented in the widely used R package PAVO (Maia *et al.*, 2019). However, inconsistency still exists in both the parameters used to characterize spectral variation, including angle dependence, and the terminology used to describe the parameters (Seago *et al.*, 2009; Galván & Sanz, 2010). This inconsistency arises because multiple parameters can be extracted from each spectral curve, and parameters that can be calculated easily for some spectra [e.g. the wavelength at maximal reflectance (Table 1) for spectra with single distinct peaks] are not meaningful for others (e.g. sigmoidal spectra). Additionally, describing optical properties integrates concepts from biology, physics and applied optics but, unfortunately, these disciplines have developed different conventions and terminology (Seago *et al.*, 2009). The present heterogeneity in measurement techniques, parameters and terminology highlights the need for a common set of measurements and parameters to enable accurate and comparable measurements between studies and species.

Here, we propose the use of a standardized set of established measurements from spectrometry to capture diffuse and specular reflection, in addition to angle-dependent properties based on the approach of Gruson *et al.* (2019a). Given that these measures capture macroscopic optical properties, they do not necessarily relate to the underlying mechanism, which is often complex and seldom known for most species (Srinivasarao, 1999; Seago *et al.*, 2009; White, 2018; Eliason *et al.*, 2020). Instead, we demonstrate that the correspondening spectral parameters can be adapted to describe any shape of spectral profile in different regions of the electromagnetic spectrum. We describe which subsets of measurements and parameters are relevant to different research questions and material properties. In addition, we propose the use of a consistent set of simple terms to enable comparison between studies, facilitate conceptual unification among disparate fields (biology and optics) and allow a clear distinction from terms used to describe colour perception (psychophysics terms). We emphasize that description of spectral properties cannot tell us about

Table 1. Glossary of selected terms related to the description and measurement of reflectance that can be found in the literature

Term	Definition	Alternative terms
Specular	Used to describe surfaces that reflect most of the light at the specular or mirror angle (same magnitude as the incident angle, but opposite direction)	–
Diffuse	Used to describe surfaces that reflect light over a wide range of angles	–
Reflectance	The proportion of light reflected by the surface at each wavelength interval. It is typically plotted on the vertical axis as a function of wavelength on the horizontal axis to represent a spectral profile and is usually reported as a percentage relative to a reflectance standard	Spectral intensity (Andersson *et al.*, 2002) Spectral reflectance (Kemp *et al.*, 2015)
Hemispherical reflectance	Light reflected from a sample over a hemisphere (2π steradians solid angle) is scattered in all directions within an integrating sphere (Fig. 1). A proportion of the scattered light is collected by a fibre-optic cable connected to a spectrometer	Overall reflectance = $2\sqrt{2\pi}B_{\max}\gamma_B$ (Gruson *et al.*, 2019b) Hemispherical/plane albedo (Hapke, 2017) Directional-hemispherical reflectance (Schaepman-Strub *et al.*, 2004)
Hemispherical directional reflectance	Light is collected from a single angle from a sample illuminated over a hemisphere (wide source). This technique was not used in our study, but we mention it here to contrast with hemispherical reflectance	Hemispherical directional (Schaepman-Strub *et al.*, 2004) Forward reflectance (Imafuku & Ogihara, 2016)
Directional reflectance	Light reflected at a specific combination of incident light and collector angles (at a specific geometry)	Bidirectional reflectance (Schaepman-Strub *et al.*, 2004; Hapke, 2017)
Specular reflectance	Directional reflectance at the specular/mirror angle: the collector and incident light are placed at equal angles but the opposite direction relative to the normal	Ordinary reflectance
Non-specular reflectance	Directional reflectance at any combination of angles other than the specular angle	–
Total reflectance	Sum of reflectance over a specified wavelength range. This term should be used instead of brightness to avoid confusion with the definition of brightness in psychophysics as the perceived intensity of light reflected by a surface (Kemp *et al.*, 2015). Note that the total reflectance can be obtained from any spectra, regardless of the geometry or technique used to capture it	Total brightness = B1 in PAVO Spectral intensity (Andersson *et al.*, 2002)
Reflectivity	The ratio of total reflected to total incident radiation, integrated over the wavelength range of interest (proportion zero to one or percentage) (Smith *et al.*, 2016b). Although, in the field of optics, reflectivity is used interchangeably with the total reflectance integrated across angles, the distinction between these two terms is particularly relevant in the field of thermal biology (Johnsen, 2012). Consequently, reflectance is wavelength resolved, whereas reflectivity as defined here is not wavelength resolved	–
Wavelength at maximal reflectance	The wavelength at which reflectance is maximal. This term, or spectral location (Table 2), should be used instead of hue to avoid confusion with the definition in psychophysics as the perceptual dimension describing the category of colour, which is not only determined by the spectral shape, but also by visual and processing features of the observer	Hue = H1 in PAVO
Gloss	Specularity that gives rise to multiple visual effects depending on the spread of reflected light around the specular angle (Franklin & Ospina-Rozo, 2021)	–

how colour is perceived by an animal, which depends on many factors, including photoreceptor sensitivities, colour opponent mechanisms and neural processing (Kemp *et al.*, 2015). However, there are many situations in which it is appropriate to characterize spectral properties independent of receiver perception. As a case study, we apply the measurements and parameters to 30 species of beetles in the scarab subfamily Rutelinae, also known as Christmas beetles, which are diverse in their optical effects. These effects can have a role in communication, camouflage and/or thermoregulation in scarabs (Thomas *et al.*, 2007; Seago *et al.*, 2009; Agez *et al.*, 2017), but their biological role for Christmas beetles has not been explored. We measure reflectance at both visible and near-infrared wavelengths, comprehensively characterize spectral properties, including angle dependence, and briefly discuss the ecological and evolutionary implications.

MATERIAL AND METHODS

GENERALIZABLE MEASUREMENTS, PARAMETERS AND TERMINOLOGY

This section describes the measurements needed to capture angle-independent and angle-dependent reflectance, in addition to the recommended terminology.

Hemispherical reflectance

We use the term hemispherical reflectance to refer to spectral measurements where reflected light is integrated across angles in a complete hemisphere. This includes both diffuse and specular reflectance (Table 1; Fig. 1); therefore, it does not provide any information regarding angle-dependent effects. It is often called total or overall reflectance (Gruson *et al.*, 2019b), but we recommend the term hemispherical reflectance to differentiate this parameter from the area under a given spectral curve, which is also generally termed total reflectance (see reflectance and total reflectance in Table 1).

Directional reflectance

We use the term directional reflectance to refer to angle-specific spectral measurements used to describe angle-dependent properties (Table 1). We distinguish two types of angle-dependent change in the spectral profile of a surface: (1) iridescence, which is an angle-dependent change in wavelength (here, we use spectral location to describe the change in wavelength; Table 2); and (2) specularity, which is an angle-dependent change in mean reflectance (Table 2). Specularity ranges from a perfect mirror, where all light is reflected

at the specular angle and none at other angles, to a perfectly diffuse surface (zero specularity), where light is reflected equally at every angle.

To analyse angle-dependent properties, it is necessary to use a spectrometer coupled to a goniometer (see schematic diagram in Supporting Information, Fig. S1) to consider multiple measurement geometries. Measurement geometry describes the specific configuration of the angle of incident light and the angle of the collector, relative to the normal (perpendicular to the sample surface). We followed the procedure proposed by Gruson *et al.* to extract the maximum information from a minimum set of measurement geometries (see detailed explanation by Gruson *et al.*, 2019a). They used two variables to describe each geometry: (1) the span, which is the angle between the direction of illumination and the direction of the collector; and (2) the bisector, which is the line that divides the span into two congruent angles (Fig. 1). Here, we use these two terms to identify the two sets of measurements (schematic diagrams in Fig. 1) to capture directional reflectance:

1. The fixed bisector set configuration captures the light reflected at the specular or mirror angle (see specular reflectance in Table 1) by keeping the bisector constant at 0° (normal to the sample) and adjusting the span to 20, 30, 40, 50 and 60°. These geometries keep the reflectance constant at the maximum to test specifically for iridescence, whereby the wavelength or spectral location shifts with the span. This assumes that the surface of the sample is parallel to the light-reflecting structure (e.g. multilayers), which might not always be the case. If the structure is heavily tilted relative to the surface of the sample, the sample tilt would need to be adjusted until reflectance is at the maximum. However, this can be time-consuming, and in many cases, it is sufficient to place the sample as flat as possible.
2. The fixed span set configuration enables comparison between specular and non-specular reflectance (Table 1), because it captures the light reflected at the specular angle and at a representative range of angles away from it. This is achieved by keeping the span constant at 20° while altering the elevation (angle with respect to the normal/zenith) of the bisector from −30 to −20, −10, 0, 10, 20 and 30° around the normal. These geometries keep the spectral location fixed while isolating the effect of specularity.

This combination of measurement geometries, originally proposed by (Gruson *et al.*, 2019a), is sufficient to describe iridescence and specularity, although it does not permit discrimination between different types of gloss (Franklin & Ospina-Rozo, 2021),
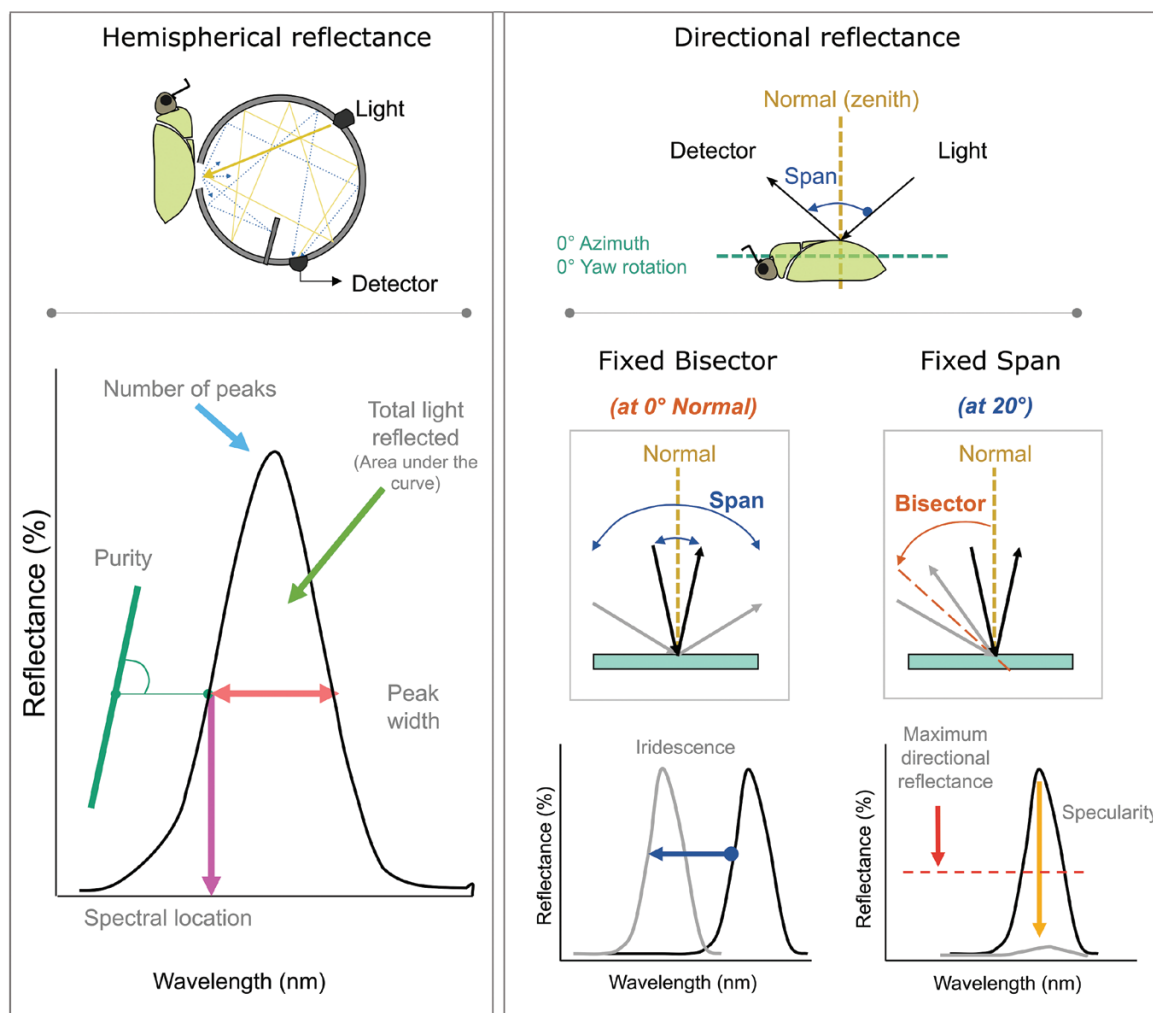
Figure 1. Methods and parameters to characterize reflectance. Top panels illustrate the measurement techniques. For hemispherical reflectance, the reflected light is integrated across angles. For directional reflectance, the span is the angle between the light and collector fibres; the bisector is the line that divides the span in half, and it can be aligned or away from the normal (zenith). The azimuth and yaw describe the alignment between the longitudinal axis of the sample and the plane of the spectrometer (for more details, see Supporting Information, Fig. S1). Left column illustrates parameters from hemispherical reflectance. The number of peaks and peak width are also represented here because they are angle independent. In the right column, the fixed bisector was used to calculate iridescence and the fixed span to calculate specularity and maximum directional reflectance (mean reflectance at the specular angle).

for which measurements at angles in very close proximity to the mirror angle are needed. Two additional parameters should be reported: the azimuth and the yaw angle (Supporting Information, Fig. S1). In our set-up, the anteroposterior longitudinal axis of the sample and the plane of the two fibres (light and collector) are aligned (azimuth = 0 and yaw = 0; Fig. 1). Rotating the sample such that its longitudinal axis is at a different angle from the plane of the spectrometer and light source would change the yaw angle. Keeping the azimuth at 0° (zenith) ensures that the equipment remains properly aligned in

this plane (see details in Supporting Information, Fig. S1). In both the fixed bisector and fixed span sets, the elevation of the light and collector probes changes. In the fixed bisector set, both probes change symmetrically, whereas in the fixed span set their position is better described by the elevation of the bisector itself (Fig. 1).

Parameters

We implemented a set of parameters based on simple statistical descriptions of spectral profiles (Fig. 1).

In order to capture the chromatic characteristics of the sample, we used the number of peaks, the spectral location (defined as the wavelength at half-maximum reflectance) and the iridescence. We used two measurements to describe saturation, namely peak width and spectral purity (a measure of curve steepness), because they vary in different ways for peaked and sigmoidal spectra (details in Table 2; examples of variability in supporting information S2 and S3). We used three different measurements to capture the achromatic properties of reflectance: the total reflectance for hemispherical reflectance, the maximum directional reflectance and the specularity (angle-dependent change in mean reflectance). All these parameters were also applied to near-infrared (NIR) reflectance. We examined the relationship between NIR and visible (VIS) wavelengths by calculating the ratio of NIR:VIS reflectance from the hemispherical reflectance measurements. The description of and rationale for each parameter, in addition to equivalent terms, are detailed in Table 2. Advantages and limitations of the parameters we have chosen in comparison to others are discussed in more detail in the Results and Discussion section. The parameters used here can be obtained directly from the widely used R package PAVO (Maia *et al.*, 2019) or calculated with simple functions (details in Table 2 and the R functions https://lospinarozo.github.io/OpticalPropertiesNaturalMaterials_RCode2021/).

The terminology we advocate for the parameters avoids using psychophysics terms related to perception, such as hue, chroma and brightness (Kemp *et al.*, 2015; Table 1). We recognize that the terms saturation and spectral purity overlap with psychophysics concepts but retain them as statistical descriptors here because they are also widely used to describe spectral characteristics independently of perception.

<div align="center">CHRISTMAS BEETLES AS A CASE STUDY</div>

Species

We studied 35 scarab beetle specimens belonging to 30 species from the subfamily Rutelinae (Scarabeidae), also known as Christmas beetles (Supporting Information, Table S1). The specimens included green, red and purple morphs of *Anoplognathus smaragdinus*, bronze and green sheen morphs of *Anoplognathus porosus* and black and green subspecies of *Repsimus manicatus*. All specimens were sourced from the Australian National Insect Collection ANIC/CSIRO (Supporting Information, Table S1).

Spectral measurements

In order to measure hemispherical reflectance, we used an integrating sphere with an inbuilt tungsten–halogen

light source (400–2100 nm; ISP-REF; Ocean Optics, Dunedin, FL, USA) and 4-mm-diameter sampling port. The integrating sphere was connected to two spectrophotometers, the USB 2000+ (400–1000 nm) and NIRQuest (1000–2100 nm), via a bifurcated optic fibre. Measurements for visible and NIR were recorded simultaneously and stitched together using the software OCEANVIEW v.1.6.7, Ocean Insight, USA before calibration. We measured one elytron on each specimen without detaching it from the body. We repeated the measurement of each sample four times on different days and averaged the results.

For directional reflectance measurements, we used the same two spectrometers as for the hemispherical reflectance measurements and two light sources: a PX-2 pulsed xenon light for the UV–visible range and HL-2000 tungsten–halogen light for the visible–NIR range (both from Ocean Optics). The spectrometers and light sources were coupled to a goniometer, allowing precise control of the angle of incident light and collector (Supporting Information, Fig. S1). The goniometer was part of a custom-designed set-up that allowed simultaneous measurement of visible and NIR reflectance over the same 1-mm-diameter spot size. The spectra from the UV–VIS and NIR spectrometers were stitched together using the software OCEANVIEW v.1.6.7. We measured one spot in a 3 mm × 3 mm piece of elytron fixed on a microscope slide. We repeated the measurement of each sample three times on different days to reduce the noise from random measurement error and averaged the results. Modifying the angles of the collector and light source inevitably alters the size of the spot (the spread of the beam changes, in addition to the area illuminated) and the optimal location of the sample. In order to account for this, every time the geometry was modified, we checked and adjusted the position of the standard and sample and recalibrated.

Choice of standards

In both cases, for hemispherical and directional reflectance we calibrated against a Lambertian 99% reflectance spectralon standard (Labsphere, North Sutton, NH, USA). Given that some of the beetles in our sample were highly specular, we frequently obtained measurements > 100% for directional reflectance measurements, particularly at the specular angle. This is because the sample reflects more light at the specular angle than the diffuse standard, which scatters the directional illumination equally across all angles. Hence, reflectance values > 100% are not problematic if all samples are compared with the same standard. For highly specular samples, a specular standard might be required to ensure a sufficient signal-to-noise ratio for accurate measurements in the fixed bisector set

Table 2. Parameters to describe reflectance properties used in this study

Parameter	Implementation	Alternative terms	Justification
Total hemispherical reflectance Integrated hemispherical reflectance (percentage reflectance × nanometres)	Area under the reflectance curve (i.e. total reflectance) calculated for the hemispherical reflectance spectrum. This measurement is wavelength resolved and integrated across angles because it is calculated from the spectra measured with an integrating sphere	Total brightness (Gruson *et al.*, 2019a) Spectral intensity (Andersson *et al.*, 2002) B1 in PAVO	Total reflectance integrated over directional reflectance measurements tends to have low repeatability. When calculating it from hemispherical reflectance, results are reliable (Supporting Information, Table S2)
Spectral location The wavelength at which reflectance is half of the maximum (in nanometres)	Wavelength at half-maximum reflectance. For a spectrum with peaks, the spectral location was always taken from the shorter-wavelength side of the peak. For a spectrum with more than one peak, we calculated this parameter for the peak with shorter wavelength. For a sigmoidal spectrum, this corresponds to the cut-off wavelength normally associated with redness. Calculated from both hemispherical and directional reflectance spectra	Hue or redness (Andersson *et al.*, 2002) $Loc = H1 - HWHM$ in PAVO instead of H3, where H1 is the wavelength at maximal location (in nanometres) and HWHM is the half-width of the peak at half-maximum reflectance (in nanometres)	Although the wavelength at maximal reflectance is useful to describe peaked spectra, it is not able to differentiate between non-saturated or sigmoidal spectra (red, brown, pink, white or yellow), for which it tends always to be 700 nm. Spectral location can be used to characterize spectra with and without peaks
Spectral purity The standardized difference between integrated reflectance on either side of the spectral location [dimensionless quantity, with range: (0:1)]	$C_{R50} = \dfrac{(R_{\lambda\,min\,-\,\lambda(R50)} - R_{\lambda(R50)\,-\,\lambda\,max})}{R_{\lambda\,min\,-\,\lambda\,max}},$ where R represents the total reflectance (area under the curve) across a given range of wavelengths and $\lambda(R50)$ = spectral location of a given sample. Values close to zero indicate lower spectral purity. In this study, we used $\lambda min = 400$ nm and $\lambda max = 700$ nm for visible light, and $\lambda min = 700$ nm and $\lambda max = 1400$ nm for NIR. This value was calculated from the hemispherical reflectance spectrum	Chroma (Andersson *et al.*, 2002) Similar parameters in PAVO: S2 (spectral saturation) and S8 (chroma) (Maia *et al.*, 2019)	This parameter was used in addition to the peak width, although they are both considered an indication of saturation. We do not consider them interchangeable, because they exhibit only weak correlation
Number of peaks [dimensionless quantity, with range: (0:2)]	We counted manually the peaks evident in most of the measurements of hemispherical and directional reflectance for each species. We did not consider a sigmoidal shape a peak; however, when a broad peak in the visible extended to the NIR, it was still considered a peak	–	We evaluated the presence of peaks based on both types of measurements (hemispherical and directional reflectance), because the integration across angles in hemispherical measurements can desaturate the spectra and mask peaks

Table 2. Continued

Parameter	Implementation	Alternative terms	Justification
Peak width Full width of the peak at half-maximum reflectance (in nanometres)	Calculated for directional reflectance spectra at 40° span. For spectra with multiple peaks, we averaged the width of the peaks. We assigned a value of zero if the number of peaks was zero	Saturation (Gruson *et al.*, 2019a) Full width at half-maximum (FWHM; in nanometres) in PAVO	This parameter is not angle dependent (Gruson *et al.*, 2019a); therefore, we measured it for only one geometry of directional reflectance. However, it can differ when calculated from hemispherical reflectance spectra because, for iridescent samples, the integration across angles gives an average reflectance that is less saturated than the directional reflectance
Iridescence Angle-dependent shift in wavelength. Here, we measured it as the angle dependence of spectral location: shift in the spectral location towards shorter wavelengths (blue shift) with an increase in the span angle (incident and observation angle) (in nanometres per 1° of span)	We fitted a linear model to describe the change in spectral location explained by the change in span. We calculated iridescence as the negative of the slope of this linear model, meaning that iridescence corresponds to the extent of blue shift. Higher values indicate more iridescence; values close to zero describe samples without iridescence, and negative values describe samples with red shifting. The term blue shift is a widely used abbreviation in the field of optics and photonics, which describes a shift of any spectra towards shorter wavelengths, and it is not restricted to spectra centred on wavelengths around 450 and 495 nm. Likewise, the term red shift refers to any shift in the spectra towards longer wavelengths	Angle dependence of hue (Gruson *et al.*, 2019a, b) Spectral richness (Deparis *et al.*, 2008)	Iridescence follows a cosine model in multilayers (Gruson *et al.*, 2019a). However, we used a linear model as a simplified statistical descriptor. The fit of a sinusoidal and linear model should be comparable for the narrow range of angles used here, and in samples with relatively simple structures (see Discussion and Supporting Information, Fig. S6). For other situations, the cosine model is more appropriate. We calculated iridescence based on spectral location, in order to be able to analyse sigmoidal spectra and to improve sensitivity for spectra with broad band peaks (see Spectral location; also Fig. 3)

Table 2. Continued

Parameter	Implementation	Alternative terms	Justification
Specularity Angle dependence of mean reflectance. A higher value means that most of the light is reflected at the specular angle (1/°)	Mean reflectance is calculated as the sum of reflectance over the wavelength range of interest divided by the number of wavelength intervals. We fitted a Gaussian model to describe the mean reflectance value explained by the position of the bisector divided by two. The model follows the equation: $D(\delta) = D_{max} \times \exp\left[-\frac{(\delta/2-t)^2}{2\gamma^2}\right]$, where D (as a percentage) is the mean reflectance at any given position of the bisector; δ (in degrees) is the position of the bisector (i.e. the difference between the angle of illumination and the angle of the collector in the study by Gruson *et al.*, 2019a); and D_{max} (as a percentage) is the maximum directional reflectance produced by the surface (at 20° span). The parameter t (in degrees) is a correction to account for the potential imperfect alignment of the structures with the surface of the sample, and γ (in degrees) indicates the spread of the reflection of the light away from the mirror angle. This term also represents the deviation or width of the Gaussian (also called 'RSM width'), named γ_B by Gruson *et al.* (2019a). We calculated specularity as $S = 1/\gamma$. High values of specularity correspond to a small spread of the reflection of the light away from the mirror angle, hence a greater drop in reflectance when the bisector moves away from the mirror angle	Angle dependence of brightness (Gruson *et al.*, 2019b). Directionality $S = 1/\gamma$ (Gruson *et al.*, 2019a, b). Gaussian model was fitted to the mean reflectance values, B2 in PAVO for each bisector angle	To estimate specularity, we used the formula for angle dependence of brightness described by Gruson *et al.* (2019a). The parameter γ_B was described originally as proportional to unspecific irregularities in multilayers. However, given that it measures the spread around the specular/mirror angle directly, it is expected to be an indicator of irregularities in any structure/natural object. For all cases, this parameter should be proportional to diffuse reflection and therefore inversely proportional to specularity
Maximum directional reflectance Maximum directional reflectance at any geometry, usually at the mirror angle (as a percentage)	The maximum value of mean reflectance that can be obtained from a surface after considering different geometries. It is likely to occur at the mirror angle. Mean reflectance is calculated as the sum of reflectance over the wavelength range of interest divided by the number of wavelength intervals. The constant D_{max} in the Gaussian model used to calculate specularity refers to the height of the peak of the curve. It is the estimate of the maximum amount of light (averaged across wavelengths, B2 in PAVO) reflected as directional reflectance by a surface. We used a function to extract the constant D_{max} at 20 span (given that our fixed span set was taken at this angle for consistency with the approach taken by Gruson *et al.*)	B_{max}(Gruson *et al.*, 2019a)	This parameter should not be confused with the maximum relative reflectance B3 obtained in PAVO, because the latter refers to the maximum value of the *y*-axis in any spectral profile. Although this value is correlated with specularity, we included it as a separate parameter because it can also be affected by absorbance and contrast gloss (Franklin & Ospina-Rozo, 2021), producing very different optical effects

Table 2. Continued

Parameter	Implementation	Alternative terms	Justification
NIR:VIS ratio Ratio of integrated reflectance in near-infrared and visible wavelengths (as a proportion)	Ratio $= \frac{R_{700\ nm-1400\ nm}}{R_{400\ nm-700\ nm}}$, where R represents the total reflectance (area under the curve) across the indicated range of wavelengths. Calculated from hemispherical reflectance	—	Given that reflectance values in VIS and NIR wavelengths are usually correlated, this measurement is useful to detect variation in relative reflectance in the two wavelength ranges

Abbreviations: NIR, near infrared; VIS, visual.

(in which all measurement geometries are specular); however, for most biological samples and non-specular measurement geometries (i.e. fixed span set), a diffuse standard is appropriate. If different standards are used for different measurements, post hoc mathematical conversions between standards can be applied.

Wavelength range and generalization

For both hemispherical and directional reflectance measurements, we excluded UV wavelengths because of the limitations of the inbuilt light source of the integrating sphere and because Christmas beetles have very low reflectance below 400 nm. However, the methods we propose here can be extended easily to UV wavelengths if required. In addition, some Christmas beetle species only reflect left-handed circularly polarized light. The equipment we used can characterize the spectral properties of this light, but not its polarization. Polarization was beyond the scope of the present study, but these methods could be extended to incorporate polarization effects by including linear or circular polarization filters placed in front of the collector and/or light source probe. We measured the optical effects at only 0° azimuth, but for experiments with samples with certain directionality (for example, hairs or scales) it might be important to take the same measurements at more than one azimuth angle.

Repeatability

We evaluated repeatability as the agreement of successive repetitions of the same measurement (details are in Supporting Information, Table S2) for the following parameters: spectral location and total hemispherical reflectance (VIS and NIR), and spectral location and mean reflectance in directional reflectance measurements. Repeatability was high for all the parameters, ranging between 0.82 and 0.99. We also calculated the standard deviation (Supporting Information, Table S2) to estimate the median and range of the variability for each parameter. Estimates for the standard deviation of the spectral location are between 1 and 4 nm in hemispherical reflectance (Supporting Information, Table S3) and between 1 and 8 nm in directional reflectance (Supporting Information, Table S4). The total reflectance varied with a median of 1.7–2.8% (SD standardized by the mean, i.e. coefficient of variation) in hemispherical reflectance (Supporting Information, Table S3), and the mean reflectance varied between 1.6 and 62% (coefficient of variation) in directional reflectance (Supporting Information, Table S5). In the latter configuration, variation can be very high for some species. These results are not owing to lack of reliability of the set-up, but attributable to the properties of the samples. Specular samples

tend to have more variation because the positioning of the sample has a considerable effect on the light collected by the collector. Our approach accounts for this variation by using a fitted value as the maximum directional reflectance, which is the amplitude of the Gaussian equation that describes the change in mean reflectance according to the measurement geometry (details and equation are in Table 2).

Application of the method and statistical analysis

In order to examine the pairwise correlations in parameters for this group of scarabs, we used Pearson's correlations between parameters for visible and NIR wavelengths separately. We visualized the differences in optical appearance between the 30 species of Christmas beetles using a principal components analysis (PCA). We conducted two independent PCAs, one for visible and one for NIR wavelengths, because we hypothesized that light manipulation in these two wavelength ranges might be subject to different selective pressures (Smith *et al.*, 2016a), and thus vary in different ways between species. The PCA enabled us to determine whether there was clustering in relationship to optical properties or taxonomy (genus).

RESULTS AND DISCUSSION

We propose a combination of measurements and parameters to enable reliable and repeatable estimates of both diffuse and specular reflection for natural materials that can be comparable across study questions and systems. The selected parameters can be applied to any spectral profile, including broadband, sigmoidal and multi-peaked spectra in different regions of the electromagnetic spectrum, which is useful for addressing non-visual functions and underlying mechanisms and for quantifying diversity (Supporting Information, Figs S2–S5). The approach advocated here combines and extends established techniques; specifically, measuring hemispherical reflectance (Johnsen, 2016), measuring directional reflectance with a goniometer (Meadows *et al.*, 2011) and implementing an optimized set of geometries to characterize angle dependence as proposed by Gruson *et al.* (2019a). The parameters are commonly used to describe spectral profiles (Montgomerie, 2006) and can be calculated using the widely used R package PAVO (Maia *et al.*, 2019). Although these parameters are statistical descriptors, they are consistent with optical principles and definitions from physics (Johnsen, 2012). We provide a standard nomenclature, consistent with recent attempts to improve uniformity of terminology in the biological literature (Kemp *et al.*, 2015; Stuart-Fox *et al.*, 2021) and with terminology used in physics

(Schaepman-Strub *et al.*, 2004; Vukusic & Stavenga, 2009; Hapke, 2017). The nomenclature is largely concordant with the names of the parameters in PAVO (Maia *et al.*, 2019); however, we propose some changes to avoid overlapping with psychophysics (Table 2).

PARAMETERS: ADVANTAGES AND LIMITATIONS

We applied the methods to describe angle dependence proposed by Gruson *et al.* (2019a), with some adaptations in order that they can be used to describe the full range of spectral profiles. First, we used spectral location rather than the wavelength of maximal reflectance and we calculated iridescence as the shift in spectral location as a function of angle, because these two measures can be applied to sigmoidal and broadband spectra. However, when using spectral location, it is important to verify that the saturation is not changing with the change in angle, otherwise desaturation could be interpreted mistakenly as iridescence. Saturation is constant in the angles of the fixed bisector set for multilayers (Gruson *et al.*, 2019a), but in other combinations of angles, or in organisms with complex, composite mechanisms, saturation should be measured.

Second, we used a linear rather than sinusoidal regression model to estimate iridescence (i.e. the shift in spectral location as a function of angle). Iridescence produced by multilayers results in a spectral shift towards shorter wavelengths with increasing angle following a cosine function (Gruson *et al.*, 2019a), although other mechanisms might produce a different pattern. For the relatively narrow range of angles considered here, the shift is approximately linear (Supporting Information, Fig. S6; Table S6). The advantage of using a linear model for non-ideal structures is that the slope is interpreted easily as the shift (in nanometres per degree). The slope also indicates the direction of the spectral shift (negative = blue shift, positive = red shift and 0 = no iridescence, whereas a sinusoidal model is not applicable to the latter two cases; Supporting Information, Fig. S6.; Table S6). However, a linear regression is not appropriate to predict spectral location beyond the interval of span angles recommended here: between 20 and 60°. Doing so would overestimate iridescence. We highlight that a cosine function (Gruson *et al.*, 2019a) is more appropriate to characterize iridescence in multilayers accurately, and a linear fit is a simplification that should be used carefully.

Third, we included two different measures of saturation, namely spectral purity and peak width. Strongly peaked spectra are highly saturated based on both measures (high spectral purity and narrow peak width), whereas high saturation for sigmoidal spectra or very broad band peaks can be characterized based

only on spectral purity. Additionally, some spectra include both sigmoidal and peaked components. One might therefore choose to use one or both of these measures depending on the spectral properties of the study system.

Lastly, we note that characterization of multi-peaked spectra is an enduring problem (McGraw, 2004; Noh *et al.*, 2010). The number of peaks was calculated manually in our study. Unfortunately, obtaining this parameter from spectra cannot be automated easily, and it is inevitably subjective because peaks (maxima) are not always clearly defined. However, we applied consistent criteria and considered a peak only if it was present in all 13 spectra for each beetle. Automation of peak identification using a machine learning or improved optimization algorithm warrants further investigation. This parameter can be excluded if the samples studied do not produce multi-peaked spectra.

MEASUREMENTS AND PARAMETERS FOR DIFFERENT RESEARCH QUESTIONS

For any given study, the appropriate choice of measurements and parameters will depend on the object properties and research question. Hemispherical reflectance is relevant for studies of thermoregulation because it represents the proportion of light (visible or near infrared) not absorbed or transmitted by the sample. This measurement can be used in studies of visual functions only if the surface is diffuse or if the goal is to contrast the main wavelengths reflected against the background. Hemispherical reflectance can be used alone if angle-dependent effects do not need to be considered in the study. Conversely, directional reflectance is useful in studies that need to consider angle-dependent visual effects, such as iridescence, gloss and intensity flashes, which have been associated with both communication and camouflage (Franklin & Ospina-Rozo, 2021; Stuart-Fox *et al.*, 2021). Directional reflectance measures comprise the fixed bisector and fixed span sets. The fixed bisector set isolates the effects of iridescence and is ideal for studies on the biological relevance of iridescence. The resulting spectral measurements can be used in visual models for studies on visual functions of iridescence (Girard & Endler, 2014; Hogan & Stoddard, 2018; Kjernsmo *et al.*, 2020). The fixed span set isolates the effect of specularity and can be used to study the biological relevance of intensity flashes, high specularity or gloss (White *et al.*, 2015; Franklin *et al.*, 2021). Lastly, NIR reflectance is relevant for thermoregulation rather than visual functions; therefore, the relevant parameters are total reflectance and the NIR:VIS ratio obtained from hemispherical reflectance (Bakken *et al.*, 1978; Medina *et al.*, 2018). Directional reflectance in NIR is relevant primarily for studies focusing on mechanisms

to reflect NIR light; for example, iridescence is a hallmark of multilayers (Starkey & Vukusic, 2013), whereas broadband, non-iridescent, non-specular NIR reflectance can be produced by disordered arrays (Johansen *et al.*, 2017).

CASE STUDY: DIVERSITY OF LIGHT MANIPULATION IN CHRISTMAS BEETLES

We have shown that the combination of techniques we used was appropriate to describe and detect different combinations of pigment-based and structural coloration in Christmas beetles, which are organisms more likely to have optical effects arising from modular complex structures rather than from ideal multilayers (Supporting Information, Figs S2–S5). For example, the hemispheric reflections of the two beetles in Figure 2 are very similar, showing a pattern associated with a pigment-based brown colour. However, they are very different in their directional reflectance profile, which shows two irregular peaks in *Anoplognathus pindarus* likely to be produced by an overlying multilayer structure. This example also highlights the utility of spectral location rather than the wavelength of maximum reflectance. The latter can easily differentiate spectra with well-defined peaks but fails to show differences for sigmoidal spectra. Spectral location is more effective in capturing these differences (Fig. 2).

We found that angle-dependent properties varied substantially among species for both visible (Fig. 3) and NIR (Fig. 4) wavelengths, altering the overall optical effect in different ways. For example, both *Anoplognathus aureus* and Calloodes frenchi have strong iridescence of ~20 nm blue shift with the change from 20 to 60° span, comparable to the iridescence of the hummingbird *Heliomaster furcifer* (~25 nm blue shift for the same change; Gruson *et al.*, 2019a). However, to the human eye, C. frenchi clearly changes from red to deep green with an increase in the viewing angle, whereas *A. aureus* does not appear to change. This effect occurs because the iridescence in C. frenchi is intensified by the presence of two peaks (both blue shifting), whereas the iridescence of *A. aureus* might be masked to the human eye by its broadband spectrum (Mitov, 2017). The gold-like metallic appearance of *A. aureus* is explained by the high degree of specularity (Fig. 3).

Another interesting example is *Anoplognathus laetus*, which appears pearlescent to the human eye: pink at the periphery and pale blue in the centre (Fig. 3). We discovered that this is the result of 'inverse iridescence', because the spectral location of *A. laetus* appears red shifted with increasing span. Inverse iridescence can be produced by a modular combination of structures (Vukusic *et al.*, 2002), but this is not the case for *A. laetus*. Instead, this beetle has a clear
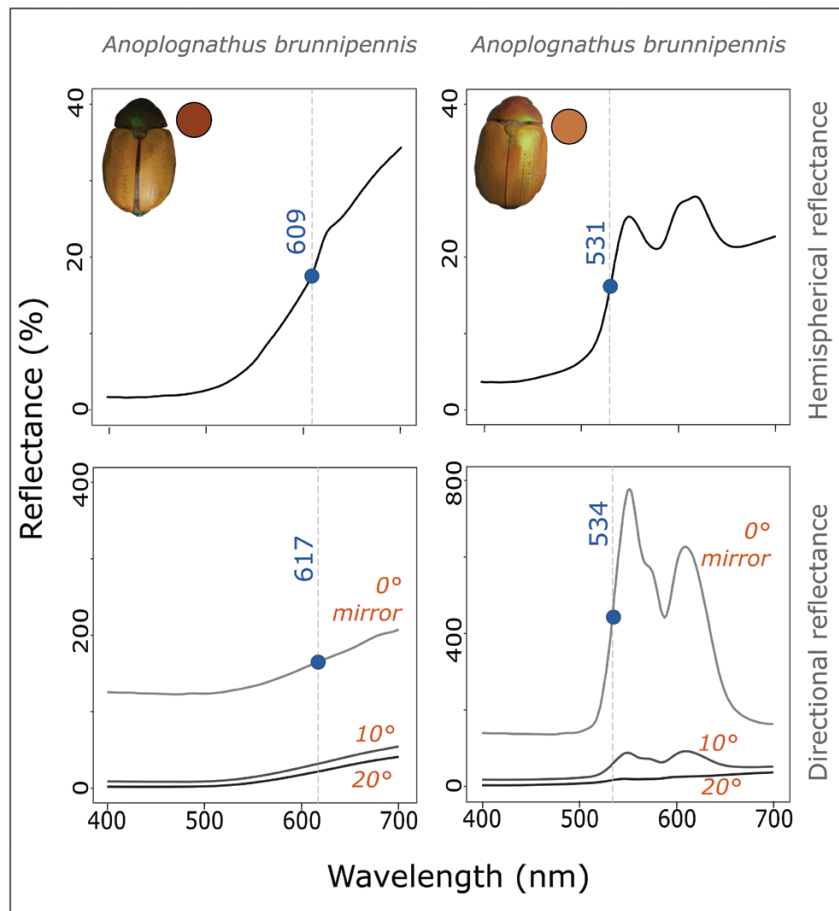
Figure 2. Example of the diversity detected by the combination of hemispherical and directional reflectance. The hemispherical reflectance profiles are similar, with reflectance increasing towards longer wavelengths. The calculated red–green–blue (RGB) colour is brown based on human vision models (circles). The directional reflectance profiles are different: *Anoplognathus brunnipennis* has a redder spectral location, and *Anoplognathus pindarus* has two clearly defined peaks with very high reflectance only at the mirror angle (bisector angle = 0, in orange). Both beetles have spectral profiles > 100% at the mirror angle. In *A. brunnipennis* this is produced by the gloss of the outer layers of wax or the epicuticle, whereas in *A. pindarus* it is produced by the specularity of the structural colour. The spectral location (blue) is more effective for capturing the difference in specular reflectance than the wavelength of maximum reflectance.

peak in reflectance in the NIR with a high degree of iridescence (Fig. 4), which gradually enters the visible spectral range as it blue shifts with increasing span, leading to a peripheral pink shade (in the areas with bigger angles in relationship to the light source). In turn, the high degree of specularity in the NIR peak of *A. laetus* explains its metallic appearance in NIR images (Fig. 4).

We used PCA to visualize the diversity of spectral properties among the 35 specimens of Christmas beetles (30 species; Fig. 5; expanded results are presented in Supporting Information, Figs S7, S8; Tables S7 and S8). The spectral properties of Christmas beetles do not cluster according to genus (Fig. 5). Species of the genus *Anoplognathus*, in particular, can achieve a great variety of combinations of the parameters we

measured. In fact, even beetles from the same species, specifically colour morphs of *Repsimus manicatus*, *A. smaragdinus* and *A. porosus*, are distant from each other in the PCA. This great variability can be explained by the fact that multiple selective pressures can determine the overall optical effects arising from the beetle elytra. Optical effects are a combination of modular pigment and structural components (Shawkey & D'Alba, 2017; Stuart-Fox *et al.*, 2021). Each of these components can be influenced directly by selection for thermoregulation, communication or camouflage, as hypothesized for the scarab *Chrysina gloriosa* (Agez *et al.*, 2017), or indirectly by selection for mechanical resistance, anti-adhesive properties or friction reduction, as shown in other beetle families (Seago *et al.*, 2009).
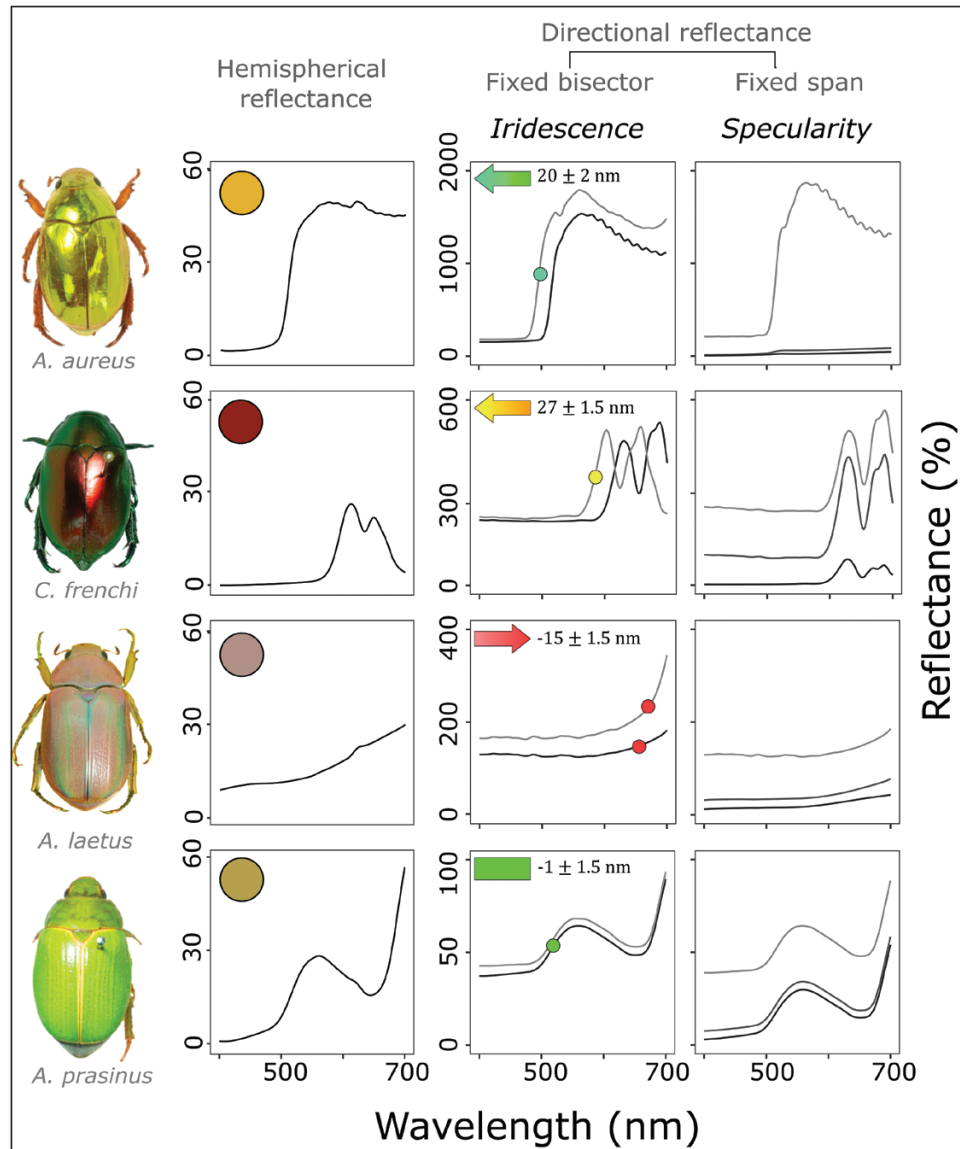
Figure 3. Diversity of angle-dependent properties. Four representative beetles are shown. The circles within the hemispherical reflectance panels show the calculated red–green–blue (RGB) colours based on human vision. The examples show different magnitudes of iridescence, reverse iridescence (red shift in *Anoplognathus laetus*) and no iridescence (*Anoplognathus prasinus*). Arrows show the direction and change (in nanometres) in spectral location (circle in the profile) in response to a change in geometry from 20° (black line) to 60° (grey line) span. The examples also show different values of specularity (note the *y*-axis). High specularity is a considerable reduction in reflectance for bisector angles other than 0° (bisector = 0° light grey, 10° dark grey and 20° black).

CORRELATION BETWEEN SPECTRAL PROPERTIES IN CHRISTMAS BEETLES

Our method enables exploration of the correlations between parameters for a given taxonomic group (Table 3). These correlations can reveal important information about potential structural or developmental constraints. For visible and NIR light, the presence of distinct peaks was associated with a shorter-wavelength spectral location, high spectral purity, iridescence and specularity (the last of these only in VIS). This is because short-wavelength or UV–blue colours are generally produced by highly ordered nanostructures that generate peaked spectra with the characteristics mentioned above (Shawkey & D'Alba, 2017). Maximum direct reflectance is expected to be proportional to specularity, because maximum reflectance is highest when all light is reflected at the specular angle (Osorio & Ham, 2002;
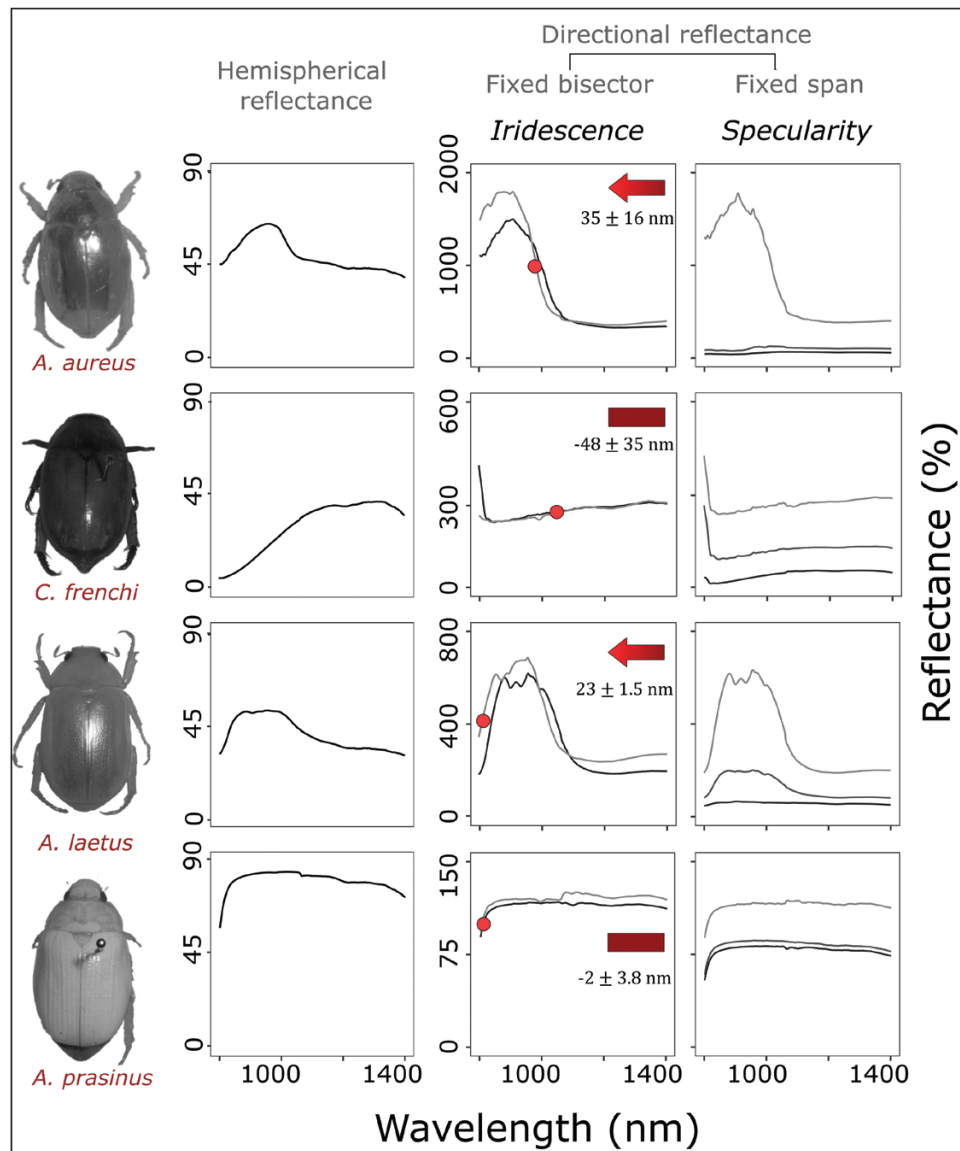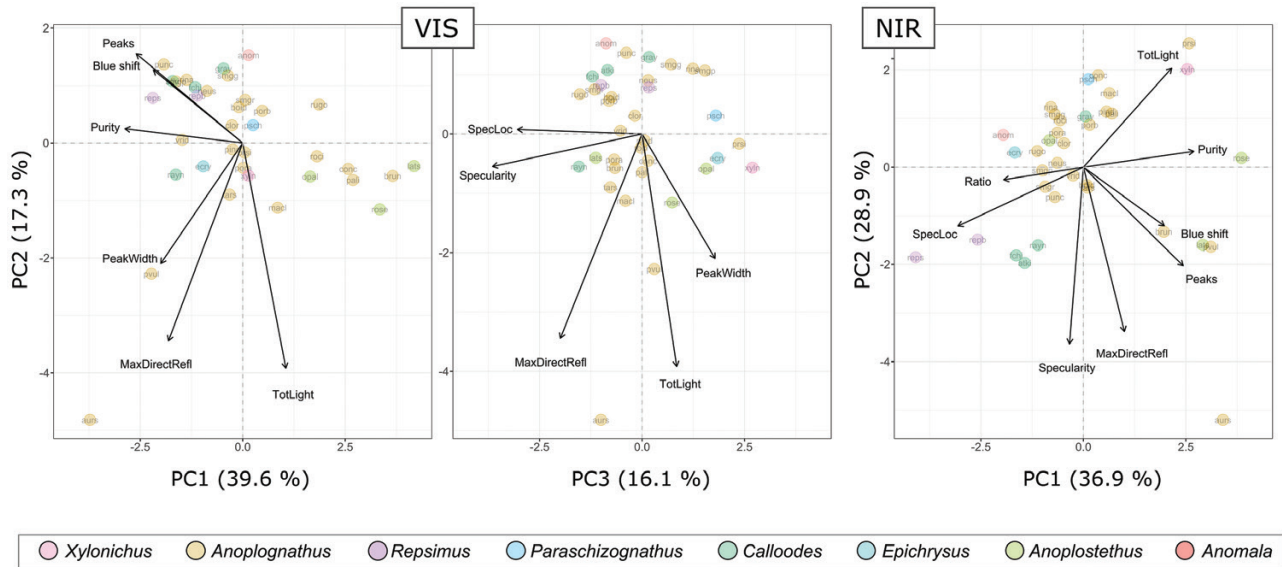
Figure 4. Diversity of near-infrared (NIR) reflectance. Near-infrared spectra of the same species as in Figure 3, with calibrated NIR photographs on the left. The examples show different magnitudes of NIR iridescence. Arrows show the direction and change (in naonometres) in spectral location (circle in the profile) in response to a change in geometry from 20° (black line) to 60° (grey line) span. The examples also show different values of specularity [considerable reduction in reflectance for bisector angles other than 0° (bisector = 0° light grey, 10° dark grey and 20° black)]. The high iridescence and specularity observed in *Anoplognathus aureus* and *Anoplognathus laetus* explain the metallic appearance of these beetles in NIR-calibrated photographs, and the broad band profile of *Anoplognathus prasinus* explains its white appearance in NIR.

Gruson *et al.*, 2019a), and our results for both NIR and VIS support this expected correlation.

Some of our results differ from the expected patterns. For instance, broadband reflection has been associated with disorder in the structure (including irregularities in the surface and chirped or chaotic multilayers) (Shawkey *et al.*, 2009; Campos-Fernández *et al.*, 2011; Cook & Amir, 2016; Johansen *et al.*, 2017; Stuart-Fox *et al.*, 2018). Therefore, it should be negatively

correlated with specularity and iridescence (Moyroud *et al.*, 2017). However, metallic appearances (mirror-like, with high distinctiveness of image; Franklin & Ospina-Rozo, 2021) combine a very broad band peak with high specularity and high maximum reflectance, as in *Anoplognathus parvulus* and *A. aureus* (Fig. 3), consistent with the phenomenon described for other gold beetles (Thomas *et al.*, 2007). In addition, beetles with an underlying broadband colour (low total

Figure 5. Multidimensional diversity of reflectance properties in Christmas beetles. Principal components analysis of the parameters used to describe visible (left and middle panels) and near-infrared (right panel) reflectance properties. Species do not group according to their genus or combinations of specific reflectance properties. Abbreviations: Blue shift, iridescence (shift towards shorter wavelengths); SpecLoc, spectral location; TotLight, total hemispherical reflectance; PeakWidth, Peak Width; MaxDirecRefl, Maximum directional reflectance; Ratio, NIR/VIS ratio.

reflectance influenced by absorption) combined with a smooth and clear overlying layer (Fig. 2) can have a sheen, white gloss or contrast gloss effect (Franklin & Ospina-Rozo, 2021) and, therefore, also high values of specularity and maximum directional reflectance. This explains the lack of negative correlation between peak width and specularity or iridescence and why higher values of maximum directional reflectance (mirror angle) can be correlated with wider peaks and high spectral purity. Overall, we did not find evidence for a strong correlation between iridescence and specularity (36% only). These properties are always strongly linked in simple, highly ordered or ideal structures (e.g. highly ordered thin films), but the correlation breaks down in biological materials owing to their modularity, complexity and the presence of different types of disorder in the structure. The causality relationships between the nanostructures and optical effects in natural materials provide an exciting and growing field, and these relationships would be worth examining in Christmas beetles, given the diversity of observed optical properties.

Total hemispherical reflectance seems to be independent of all other properties. However, we found an inverse correlation with the number of peaks for visible light, possibly because a broadband flat spectrum (light brown or white) has higher total reflected light than highly saturated peaks. Conversely, for NIR reflectance, we found a strong correlation between total hemispherical reflectance and shorter-wavelength spectral location, higher spectral purity and low specularity. This might be attributable to the presence of multiple cases of sigmoidal NIR reflectance at wavelengths < 1400 nm. This corresponds to the spectral power distribution of sunlight and would ensure reflection of a high proportion of the energy in sunlight if NIR reflection was used for thermoregulation. The NIR:VIS ratio exhibits a negative correlation with the total hemispherical reflectance in the NIR, suggesting that highly reflective beetles tend to have broad reflectance across both spectral ranges.

ECOLOGICAL AND EVOLUTIONARY IMPLICATIONS

Visualizing the multidimensional diversity of optical effects along with the correlations between different parameters can provide insights into whether certain optical properties tend to evolve together because of phylogenetic relationships, structural or developmental constraints or because they serve similar purposes. Some of the correlations we observed were weaker than expected from optical theory of ideal structures, highlighting the complexity and modularity of natural structures and suggesting that different parameters might be influenced by different selective pressures. For example, the iridescence and specularity in the visible range could be important

Table 3. Correlations between parameters that describe visible and near-infrared reflectance

Parameter	Spectral location		Peak width		Total hemispherical reflectance		Spectral purity		Blue shift		Specularity		Maximum directional reflectance		NIR:VIS ratio
	VIS	NIR	VIS	NIR	VIS	NIR	VIS	NIR	VIS	NIR	VIS	NIR	VIS	NIR	NIR
Number of peaks	-0.34*	-0.47*	0.37*	NA	-0.39*	0.08	0.60*	0.53*	0.58*	0.54*	0.37*	0.31	0.2	0.58*	-0.27
Spectral location	–	–	-0.32	NA	0.09	-0.71*	-0.71*	-0.77*	-0.16	-0.28	-0.13	0.35*	-0.16	-0.05	0.51*
Peak width	–	–	–	–	0.07	NA	0.54*	NA	0.19	NA	0.1	NA	0.45*	NA	NA
Total hemispherical reflectance	–	–	–	–	–	–	-0.27	0.46*	-0.24	0.09	-0.26	-0.43*	0.25	-0.11	-0.36*
Spectral purity	–	–	–	–	–	–	–	–	0.47*	0.33*	0.28	-0.13	0.32*	0.14	-0.09
Blue shift	–	–	–	–	–	–	–	–	–	–	0.36*	0.11	0.22	0.25	-0.36*
Specularity	–	–	–	–	–	–	–	–	–	–	–	–	0.62*	0.82*	0.08
Maximum directional reflectance	–	–	–	–	–	–	–	–	–	–	–	–	–	–	-0.10

Values are the Pearson's correlation coefficients. Iridescence is reported here as the magnitude of the blue shift in spectral location.
*$P < 0.05$.
Abbreviation: NA, not assessed; NIR, near infrared; VIS, visual.

for communication or camouflage (Vukusic *et al.*, 2002; Kemp & Rutowski, 2007; Schultz & Fincke, 2009; Kjernsmo *et al.*, 2018, 2020), whereas the total hemispherical reflectance and NIR reflectance could be associated with thermoregulation (Bakken *et al.*, 1978; Smith *et al.*, 2016a; Stuart-Fox *et al.*, 2017; Medina *et al.*, 2018). To elucidate biological function, the diversity of optical properties observed in Christmas beetles needs to be investigated in the context of the habitat and behaviour of the beetles. Additionally, the great diversity of optical properties we observed in closely related species raises fascinating questions regarding the development and evolution of underlying mechanisms, such as whether they are evolutionarily labile or constrained by trade-offs (e.g. Maia *et al.*, 2016; Babarovic *et al.*, 2019; Nordén *et al.*, 2021; Lloyd & Nadeau, 2021).

Standardized methods, parameters and terminology will facilitate comparison between studies and species, and the incorporation of angle dependence and NIR measurements will be likely to reveal new adaptations. Specular and diffuse reflectance and angle dependence could be incorporated into models of animal colour vision (Endler & Mielke, 2005; Simpson & McGraw, 2018; White, 2020) to ask questions about appearance to different receivers, including conspecifics, predators and prey, and how appearance changes depending on the geometry of illumination and viewing (Simpson & McGraw, 2018; Echeverri *et al.*, 2021). Currently, we have limited understanding of how iridescence and specularity are perceived and processed by different animals and whether they might have different biological functions, largely because of the previous lack of methods to study them separately (Doucet & Meadows, 2009; Morehouse & Rutowski, 2009; Stuart-Fox *et al.*, 2021). Our hope is that the approach discussed here to quantify the angle dependence of chromatic and achromatic components independently will stimulate research into their biological function. Finally, our results also revealed diversity in NIR directional reflectance, which raises questions regarding similarities and differences in the underlying mechanism among species and whether this diversity represents adaptive variation. Further studies are required to understand the biological relevance of directional reflectance and NIR light manipulation.

ACKNOWLEDGEMENTS

DATA AVAILABILITY

The data underlying this article are available in the Dryad Digital Repository at https://doi.org/10.5061/dryad.2v6wwpznp (Ospina-Rozo *et al.*, 2022). The online interactive version of our code can be found as a GitHub page here: https://lospinarozo.github.io/OpticalPropertiesNaturalMaterials_RCode2021/.

REFERENCES

Agez G, **Bayon C**, **Mitov M. 2017.** Multiwavelength micromirrors in the cuticle of scarab beetle *Chrysina gloriosa*. *Acta Biomaterialia* **48:** 357–367.

Andersson S, **Pryke SR**, **Ornborg J**, **Lawes MJ**, **Andersson M. 2002.** Multiple receivers, multiple ornaments, and a trade-off between agonistic and epigamic signaling in a widowbird. *The American Naturalist* **160:** 683–691.

Babarovic F, **Puttick MN**, **Zaher M**, **Learmonth E**, **Gallimore EJ**, **Smithwick FM**, **Mayr G**, **Vinther J. 2019.** Characterization of melanosomes involved in the production of non-iridescent structural feather colours and their detection in the fossil record. *Journal of the Royal Society Interface* **16:** 20180921.

Bakken GS, **Vanderbilt VC**, **Buttemer WA**, **Dawson WR. 1978.** Avian eggs: thermoregulatory value of very high near-infrared reflectance. *Science* **200:** 321–323.

Campos-Fernández C, **Azofeifa DE**, **Hernández-Jiménez M**, **Ruiz-Ruiz A**, **Vargas WE. 2011.** Visible light reflection spectra from cuticle layered materials. *Optical Materials Express* **1:** 85–100.

Cook CQ, **Amir A. 2016.** Theory of chirped photonic crystals in biological broadband reflectors. *Optica* **3:** 1436–1439.

Cuthill IC, **Allen WL**, **Arbuckle K**, **Caspers B**, **Chaplin G**, **Hauber ME**, **Hill GE**, **Jablonski NG**, **Jiggins CD**, **Kelber A**, **Mappes J**, **Marshall J**, **Merrill R**, **Osorio D**, **Prum R**, **Roberts NW**, **Roulin A**, **Rowland H**, **Sherratt TH**, **Skelhorn J**, **Speed MP**, **Stevens M**, **Stoddard MC**, **Stuart-Fox D**, **Talas L**, **Tibbetts E**, **Caro T. 2017.** The biology of colour. *Science* **357:** 6350.

Cuthill IC, **Bennett ATD**, **Partridge JC**, **Maier EJ. 1999.** Plumage reflectance and the objective assessment of avian sexual dichromatism. *The American Naturalist* **160:** 183–200.

Deparis O, **Rassart M**, **Vandenbem C**, **Welch V**, **Vigneron JP**, **Lucas S. 2008.** Structurally tuned iridescent

surfaces inspired by nature. *New Journal of Physics* **10:** 013032.

Doucet SM, **Meadows MG. 2009.** Iridescence: a functional perspective. *Journal of the Royal Society Interface* **6:** S115–S132.

Echeverri SA, **Miller AE**, **Chen J**, **McQueen EW**, **Plakke M**, **Spicer M**, **Hoke KL**, **Stoddard MC**, **Morehouse NI. 2021.** How signaling geometry shapes the efficacy and evolution of animal communication systems. *Integrative and Comparative Biolology* **61:** 787–813.

Eliason CM, **Maia R**, **Parra JL**, **Shawkey MD. 2020.** Signal evolution and morphological complexity in hummingbirds (Aves: Trochilidae). *Evolution; international journal of organic evolution* **74:** 447–458.

Endler JA. 1990. On the measurement and classification of colour in studies of animal colour patterns. *Biological Journal of the Linnean Society* **41:** 315–352.

Endler JA, **Mielke PW Jr. 2005.** Comparing entire colour patterns as birds see them. *Biological Journal of the Linnean Society* **86:** 405–431.

Franklin AM, **Ospina-Rozo L. 2021.** Gloss. *Current Biology* **31:** R172–R173.

Franklin AM, **Rankin KJ**, **Ospina Rozo L**, **Medina I**, **Garcia JE**, **Ng L**, **Dong C**, **Wang L-Y**, **Aulsebrook AE**, **Stuart-Fox D. 2021.** Cracks in the mirror hypothesis: High specularity does not reduce detection or predation risk. *Functional Ecology* **36:** 239–248.

Fu J, **Yoon BJ**, **Park JO**, **Srinivasarao M. 2017.** Imaging optical scattering of butterfly wing scales with a microscope. *Interface Focus* **7:** 20170016.

Galván I, **Sanz JJ. 2010.** Measuring plumage colour using different spectrophotometric techniques: a word of caution. *Ornis Fennica* **87:** 87–89.

Girard MB, **Endler JA. 2014.** Peacock spiders. *Current Biology* **24:** R588–R590.

Gruson H, **Andraud C**, **Daney de Marcillac W**, **Berthier S**, **Elias M**, **Gomez D. 2019a.** Quantitative characterization of iridescent colours in biological studies: a novel method using optical theory. *Journal of the Royal Society Interface Focus* **9:** 20180049.

Gruson H, **Elias M**, **Andraud C**, **Djediat C**, **Berthier S**, **Doutrelant C**, **Gomez D. 2019b.** Hummingbird iridescence: an unsuspected structural diversity influences colouration at multiple scales. *bioRxiv* 699744.

Hapke B. 2017. Reflectance methods and applications. *Encyclopedia of spectroscopy and spectrometry*, *3rd edn*. Oxford: Academic Press, 931–935.

Hogan BG, **Stoddard MC. 2018.** Synchronization of speed, sound and iridescent color in a hummingbird aerial courtship dive. *Nature Communications* **9:** 5260.

Imafuku M, **Ogihara N. 2016.** Wing scale orientation alters reflection directions in the green hairstreak *Chrysozephyrus smaragdinus* (Lycaenidae; Lepidoptera). *Zoological Science* **33:** 616–622.

Johansen VE, **Onelli OD**, **Steiner LM**, **Vignolini S. 2017.** Photonics in nature: from order to disorder. In: Gorb S, Gorb E, eds. *Functional Surfaces in Biology III*, *1st edn*. Cham: Springer International, 53–89.

Johnsen S. 2012. *The optics of life: a biologist's guide to light in nature*. Princeton, New Jersey, USA: Princeton University Press.

Johnsen S. 2016. How to measure color using spectrometers and calibrated photographs. *Journal of Experimental Biology* **219:** 772–778.

Kemp DJ, **Herberstein ME**, **Fleishman LJ**, **Endler JA**, **Bennett AT**, **Dyer AG**, **Hart NS**, **Marshall J**, **Whiting MJ. 2015.** An integrative framework for the appraisal of coloration in nature. *The American Naturalist* **185:** 705–724.

Kemp DJ, **Rutowski RL. 2007.** Condition dependence, quantitative genetics, and the potential signal content of iridescent ultraviolet butterfly coloration. *Evolution; international journal of organic evolution* **61:** 168–183.

Kinoshita S, **Yoshioka S**, **Kawagoe K. 2002.** Mechanisms of structural colour in the *Morpho* butterfly: cooperation of regularity and irregularity in an iridescent scale. *Proceedings of the Royal Society B: Biological Sciences* **269:** 1417–1421.

Kjernsmo K, **Hall JR**, **Doyle C**, **Khuzayim N**, **Cuthill IC**, **Scott-Samuel NE**, **Whitney HM. 2018.** Iridescence impairs object recognition in bumblebees. *Scientific Reports* **8:** 8095.

Kjernsmo K, **Whitney HM**, **Scott-Samuel NE**, **Hall JR**, **Knowles H**, **Talas L**, **Cuthill IC. 2020.** Iridescence as camouflage. *Current Biology* **30:** 551–555.e3.

Lloyd VJ, **Nadeau NJ. 2021.** The evolution of structural colour in butterflies. *Current Opinion in Genetics and Development* **69:** 28–34.

Maia R, **Gruson H**, **Endler JA**, **White TE. 2019.** PAVO 2: new tools for the spectral and spatial analysis of colour in R. *Methods in Ecology and Evolution* **10:** 1097–1107.

Maia R, **Rubenstein DR**, **Shawkey MD. 2016.** Selection, constraint, and the evolution of coloration in African starlings. *Evolution; international journal of organic evolution* **70:** 1064–1079.

McGraw KJ. 2004. Multiple UV reflectance peaks in the iridescent neck feathers of pigeons. *Naturwissenschaften* **91:** 125–129.

Meadows MG, **Butler MW**, **Morehouse NI**, **Taylor LA**, **Toomey MB**, **McGraw KJ**, **Rutowski RL. 2009.** Iridescence: views from many angles. *Journal of the Royal Society Interface* **6:** S107–S113.

Meadows MG, **Morehouse NI**, **Rutowski R L**, **Douglas JM**, **McGraw KJ. 2011.** Quantifying iridescent coloration in animals: a method for improving repeatability. *Behavioral Ecology and Sociobiology* **65:** 1317–1327.

Medina I, **Newton E**, **Kearney MR**, **Mulder RA**, **Porter WP**, **Stuart-Fox D. 2018.** Reflection of near-infrared light confers thermal protection in birds. *Nature Communications* **9:** 3610.

Mitov M. 2017. Cholesteric liquid crystals in living matter. *Soft Matter* **13:** 4176–4209.

Montgomerie R. 2006. Analyzing colors. In: Hill GE, McGraw KJ, eds. *Bird coloration, volume I: mechanisms and measurements*. Cambridge: Harvard University Press, 90–147.

Morehouse NI, **Rutowski RL. 2009.** Comment on 'Floral iridescence, produced by diffractive optics, acts as a cue for animal pollinators'. *Science* **325:** 1072; author reply 1072.

Moyroud E, **Wenzel T**, **Middleton R**, **Rudall PJ**, **Banks H**, **Reed A**, **Mellers G**, **Killoran P**, **Westwood MM**, **Steiner U**,

Vignolini S, **Glover BJ. 2017.** Disorder in convergent floral nanostructures enhances signalling to bees. *Nature* **550:** 469–474.

Noh H, **Liew SF**, **Saranathan V**, **Prum RO**, **Mochrie SGJ**, **Dufresne ER**, **Cao H. 2010.** Double scattering of light from biophotonic nanostructures with short-range order. *Optics Express* **18:** 11942–11948.

Nordén KK, **Eliason CM**, **Stoddard MC. 2021.** Evolution of brilliant iridescent feather nanostructures. *eLife* **10:** e71179.

Osorio D, **Ham AD. 2002.** Spectral reflectance and directional properties of structural coloration in bird plumage. *The Journal of Experimental Biology* **205:** 2017–2027.

Osorio D, **Vorobyev M. 2008.** A review of the evolution of animal colour vision and visual communication signals. *Vision Research* **48:** 2042–2051.

Ospina-Rozo L, **Roberts A**, **Stuart-Fox D. 2022.** Data and original code from: A generalized approach to characterise optical properties of natural objects. *Dryad Database*. doi: 10.5061/dryad.2v6wwpznp.

Schaepman-Strub G, **Painter T**, **Huber S**, **Dangel S**, **Schaepman ME**, **Martonchik J**, **Berendse F. 2004.** About the importance of the definition of reflectance quantities-results of case studies. In M.O. Altan (Ed.), XXth ISPRS Congress (pp. 361-366). Istanbul, Turkey.

Schultz TD, **Fincke OM. 2009.** Structural colours create a flashing cue for sexual recognition and male quality in a Neotropical giant damselfly. *Functional Ecology* **23:** 724–732.

Seago AE, **Brady P**, **Vigneron JP**, **Schultz TD. 2009.** Gold bugs and beyond: a review of iridescence and structural colour mechanisms in beetles (Coleoptera). *Journal of the Royal Society Interface* **6:** S165–S184.

Shawkey MD, **D'Alba L. 2017.** Interactions between colour-producing mechanisms and their effects on the integumentary colour palette. *Philosophical Transactions of the Royal Society B: Biological Sciences* **372:** 20160536.

Shawkey MD, **Morehouse NI**, **Vukusic P. 2009.** A protean palette: colour materials and mixing in birds and butterflies. *Journal of the Royal Society Interface* **6:** S221–S231.

Simpson RK, **McGraw KJ. 2018.** It's not just what you have, but how you use it: solar-positional and behavioural effects on hummingbird colour appearance during courtship. *Ecology Letters* **21:** 1413–1422.

Smith KR, **Cadena V**, **Endler JA**, **Kearney MR**, **Porter WP**, **Stuart-Fox D. 2016a.** Color change for thermoregulation versus camouflage in free-ranging lizards. *The American Naturalist* **188:** 668–678.

Smith KR, **Cadena V**, **Endler JA**, **Porter WP**, **Kearney MR**, **Stuart-Fox D. 2016b.** Colour change on different body regions provides thermal and signalling advantages in bearded dragon lizards. *Proceedings of the Royal Society B: Biological Sciences* **283:** 20160626.

Srinivasarao M. 1999. Nano-optics in the biological world: beetles, butterflies, birds, and moths. *Chemical Reviews* **99:** 1935–1962.

Starkey T, **Vukusic P. 2013.** Light manipulation principles in biological photonic systems. *Nanophotonics* **2:** 289–307.

Stavenga DG, **Leertouwer HL**, **Marshall NJ**, **Osorio D. 2011.** Dramatic colour changes in a bird of paradise caused by uniquely structured breast feather barbules. *Proceedings of the Royal Society B: Biological Sciences* **278:** 2098–2104.

Stuart-Fox D, **Moussalli A. 2009.** Camouflage, communication and thermoregulation: lessons from colour changing organisms. *Philosophical Transactions of the Royal Society B: Biological Sciences* **364:** 463–470.

Stuart-Fox D, **Newton E**, **Clusella-Trullas S. 2017.** Thermal consequences of colour and near-infrared reflectance. *Philosophical Transactions of the Royal Society B: Biological Sciences* **372:** 20160345.

Stuart-Fox D, **Newton E**, **Mulder RA**, **D'Alba L**, **Shawkey MD**, **Igic B. 2018.** The microstructure of white feathers predicts their visible and near-infrared reflectance properties. *PLoS One* **13:** e0199129.

Stuart-Fox D, **Ospina-Rozo L**, **Ng L**, **Franklin AM. 2021.** The paradox of iridescent signals. *Trends in Ecology & Evolution* **36:** 187–195.

Thomas DB, **Seago A**, **Robacker DC. 2007.** Reflections on golden scarabs. *American Entomologist* **53:** 224–230.

Vignolini S, **Moyroud E**, **Glover BJ**, **Steiner U. 2013.** Analysing photonic structures in plants. *Journal of the Royal Society Interface* **10:** 20130394.

Vukusic P, **Sambles JR**, **Lawrence CR**, **Wootton RJ. 2002.** Limited-view iridescence in the butterfly *Ancyluris meliboeus*. *Proceedings of the Royal Society B: Biological Sciences* **269:** 7–14.

Vukusic P, **Stavenga DG. 2009.** Physical methods for investigating structural colours in biological systems. *Journal of the Royal Society Interface* **6:** S133–S148.

White TE. 2018. Illuminating the evolution of iridescence. *Trends in Ecology & Evolution* **33:** 374–375.

White TE. 2020. Structural colours reflect individual quality: a meta-analysis. *Biology Letters* **16:** 20200001.

White TE, **Zeil J**, **Kemp DJ. 2015.** Signal design and courtship presentation coincide for highly biased delivery of an iridescent butterfly mating signal. *Evolution; international journal of organic evolution* **69:** 14–25.

Wilts BD, **Leertouwer HL**, **Stavenga DG. 2009.** Imaging scatterometry and microspectrophotometry of lycaenid butterfly wing scales with perforated multilayers. *Journal of the Royal Society Interface* **6:** S185–S192.

SUPPORTING INFORMATION

Additional Supporting Information may be found in the online version of this article at the publisher's web-site.

Table S1. Specimens used in this research and their accession number or label information for unregistered specimens. All specimens were obtained from the Australian National Insect Collection (ANIC).

Table S2. Repeatability for basic parameters used in describing spectral curves.

Table S3. Variability in the parameters describing the hemispherical reflectance spectra. We calculated the variability as the standard deviation (in nanometres) for the spectral location parameter, and the coefficient of variation (standard deviation normalized by the mean of the parameter; CV; as a percentage). The variability is relatively low, as shown by the median of the variation for each parameter.

Table S4. Standard deviation in spectral location of the directional reflectance spectra in different span angles (in nanometres). The variation is generally low (median = 1.15 nm, minimum = 0 nm, maximum = 8.54 nm), meaning that the parameter is reliable.

Table S5. Coefficient of variation (as a percentage) of the mean reflectance of the directional reflectance spectra in different bisector angles (in nanometres).

Table S6. Comparison between the parameters in cosine (Gruson *et al.*, 2019a) and linear models, where *Y* is the spectral location at a given angle (in nanometres), and *x* is the span angle (in degrees).

Table S7. Results of the principal components analysis for visible (VIS) light, showing the percentage of variance explained by the first three components. The cumulative proportion of variance explained is 74.8% (highlighted in blue).

Table S8. Results of the principal components analysis for near-infrared (NIR) light, showing the percentage of variance explained by the first three components. The cumulative proportion of variance explained by principal components PC1 and PC2 is 68.2% (highlighted in red).

Figure S1. Three-dimensional planes describing our goniometer set-up to measure directional reflectance. A goniometer allows different combinations of angles for the incident light and the collector. We use the axes of a beetle to illustrate the three dimensions (circle). In our set-up, the light and the collector are always aligned in the plane of the anteroposterior longitudinal axis of the sample, which means they are always at 0° azimuth. The position of the sample must be adjusted to the optimal distance for the light and collector to be in focus, which is signalled by the focal plane of a customized camera attached to the collector. The changes in the bisector and span angle cause changes in the elevation of both light and collector. We adjust the rotation in pitch and roll to ensure that the sample is as flat as possible. Changing the azimuth angle (front view) is not desirable because it might result in an angled surface or alignment issues. Changing the yaw rotation might be informative and should always be reported, because the optical properties might differ with different yaw angles in non-symmetric structures. In our experiment, we measured all our samples at 0° yaw.

Figure S2. Green diversity. These four green beetles have very different spectral profiles in the visible directional reflectance. In all cases, the geometries compared are span at 20° and span at 60° in the fixed bisector set. The four beetles show a shift towards shorter wavelengths with the increase in span angle, which corresponds to iridescence.

Figure S3. Sheen. These four green beetles have a brown background with a topcoat shiny sheen, which is visible at only certain angles. Thus, in order to compared them, we used the fixed span set, with the bisector at 0° (centred in the normal) and bisector at 20°. The optical properties of the sheen are detectable only when measuring at the specular angle, and they vary considerably between species. The measurements away from the normal describe the properties of the brown background.

Figure S4. Iridescent near infrared (NIR). These four beetles have defined peaks in the NIR, and all of them show a shift towards shorter wavelengths with the increase in span angle, which corresponds to iridescence. In all cases, the geometries compared are span at 20° and span at 60° in the fixed bisector set.

Figure S5. Diffuse near infrared (NIR). These four beetles have a high NIR reflectance with a plateau. In these cases, the geometry is the span at 20° in the fixed bisector set.

Figure S6. Examples of the application of linear vs. sinusoidal models. For *Anoplognathus smaragdinus* (red, green and blue morph), the two models behave in a similar manner in the range of angles that we studied. For span angles < 20°, the linear model overestimates the spectral location, hence overestimating the iridescence. However, for species with a red shift (top right) or without any angle dependence in the spectra (bottom right), a sinusoidal model is not able to describe the pattern. The red shift in *Anoplognathus laetus* and *Anoplognathus brunnipennis* is produced by the presence of an iridescent peak in the near infrared (NIR; see Figs 3, 4). Although the pattern in the NIR could be explained by a sinusoid, not all studies are able to measure NIR or interested in doing so. Instead, linear models allow the simplest and most easily interpretable comparison between beetles with different degrees of angle-dependent shifting of the spectra.

Figure S7. Results of principal components analysis. A, scree plot. Only the first three principal components (PCs) have eigenvalues greater than one, hence we consider only these three. B, loadings matrix. Correlations between spectral parameters and the first three PCs. Scale bar: significant correlations (beyond −0.3 to +0.3 range) are shaded in colours. Principal component 1 is negatively correlated with spectral purity, number of peaks

and iridescence (as blue shift). Principal component 2 is strongly correlated with the total light reflected and the maximum directional reflectance. Principal component 3 is positively correlated with specularity and spectral location but negatively with peak width.

Figure S8. Results of principal components analysis. A, scree plot. Only the first two principal components (PCs) have eigenvalues greater than one, hence we consider only these two. B, loadings matrix. Correlations between spectral parameters and the first three PCs (owing to the eigenvalue of PC3 being close to one). Scale bar: significant correlations (beyond −0.3 to +0.3 range) are shaded in colours. Principal component 1 is positively correlated with the number of peaks, spectral purity and iridescence (as blue shift) and negatively with spectral location and ratio of near-infrared to visible (NIR:VIS). Principal component 2 is positively correlated with the total light reflected and negatively with specularity and the maximum directional reflectance.